Microwave Review
December 2024, Vol. 30, No. 2, pp. 129-136
DOI: 10.18485/mtts_mr.2024.30.2.15

Photonics Crystal Fiber for Salinity Sensing Applications with A Large Negative Dispersion

Ilhem Mired[1], Hichem Chikh-Bled[2], Mohammed Debbal[3]

Abstract – **In this study, we propose a novel approach to enhance the sensitivity of salinity measurement using photonic crystal fiber. Our method involves filling the first ring of holes in the fiber with seawater, which serves as the analyte, and embedding it in a single-material silica substrate. This design allows for precise tuning of sensitivity to even minimal changes in salinity concentration. Through numerical simulations, we explore the influence of different geometrical parameters on the photonic crystal fiber's (PCF) characteristics. We calculate the sensitivity for two wavelengths, 1.3µm and 1.55µm, and achieve a highest salinity sensitivity of 0.017966 ps/(nm·km)/PSU and 0.021818 ps/(nm·km)/PSU, respectively. Our proposed sensor not only demonstrates excellent performance in salinity sensing but also holds promise for applications in the field of communication, thanks to its satisfactory and impressive sensing capabilities.**

Keywords – **Photonic Crystal Fiber (PCF), Chromatic Dispersion, Sensitivity, Salinity sensor.**

I. INTRODUCTION

For decades, electrical sensors have been the preferred method for detecting mechanical and physical phenomena [1]. These sensors are widely used, although they have built-in limitations such transmission loss [2] and sensitivity to electromagnetic interference (noise) [3], which make their use difficult, if not impossible, in many applications. Optical sensing provides an excellent solution to these challenges, using light instead of electricity and fiber optics instead of copper wire [4]. Optical fiber sensors now have more capabilities thanks to lower component costs and higher component quality [5] to replace conventional sensors using. The majority of commercially viable optical fiber sensors in the early days of the technology were directed directly at markets where the available sensor technology was insufficient or marginal. The fundamental advantages of optical fiber sensors such as their light weight, compact size, passivity, low power and resistance to radio frequency interference, high sensitivity, bandwidth, environmental resistance, and environmental robustness, were frequently employed to make up for their primary disadvantages of being expensive and unfamiliar to the end user. Sensors based optical fiber are devices widely used in many fields, from environmental monitoring [6] to the medical industry [7].

Article history: Received Month dd, yyyy; Accepted Month dd, yyyy

[1]Ilhem Mired is with Smart Structure Laboratory (SSL), University of Ain Temouchant, Algeria, E-mail: ilhem.mired@univ-temouchent.edu.dz

[2]Hicham Chikh-Bled is with University of Tlemcen, Algeria, E-mail: hicham.chikhbled@gmail.com

[3]Mohammed Debbal are with University of Ain Temouchant, Algeria, E-mail: mohammed.debbal@univ-temouchent.edu.dz

Comparing photonic crystal fiber (PCF) to conventional optical fiber, this latter has a better geometry. Typically, PCF has a hollow or solid core that is surrounded by variously sized airholes. The arrangement of these airholes controls the light [8]. In addition, by changing the location of the airholes as well as the surrounding conditions, light propagation can be controlled. In recent decades, PCF has gained significant attention in sensing applications due to its distinct characteristics. Numerous research groups are interested in PCF based sensors because of its great sensitivity [9], flexibility [10], small size, robustness and the fact that they can be used in measurement applications. They can also be utilized in risky, noisy, high-temperature, and high-voltage settings, with high electromagnetic fields and in explosive environments [11], even for remote supervision and remote sensing applications [12]. Their ability to transmit and manipulate light precisely makes them versatile tools for detecting and measuring a variety of physical or chemical quantities like pressure [13], temperature [14], PH [15], DNA [16], Cholesterol [17], glucose [18], rotation [19], acceleration [20], measurement of electric and magnetic fields [21], acoustics [22], vibration [23], linear and angular position [24], deformation [25], humidity [26], viscosity [27], chemical measurement [28], water salinity [29] and a host of other sensor applications. Salinity is an essential variable in oceanography since it indicates how the marine environment is doing [30]. Salinity sensors are crucial for managing production procedures and safeguarding ecosystems [31]. One of the key intrinsic optical qualities of seawater is its optical index of refraction.

Sensors relying on polyimide-coated photonic crystal fiber have been described [32]. A photonic crystal fiber salinity sensor was investigated [29]. A seawater salinity sensor based on a dual-core photonic circuit and using a tiny fiber-optic probe has been the subject of theoretical and numerical analysis [30] and Sagnac interferometer-based ultrahigh sensitivity photonic crystal fiber (PCF) salinity sensor was presented [33].

We explored a salinity sensor using photonic crystal fiber. However, an important issue arises in the current research: the variation of the chromatic dispersion by varying the concentrations of salt in water at a specific wavelength, which are not addressed in previous works. When deploying this sensor in marine and groundwater environments, it's crucial to consider the wavelength and the dispersion alongside the salt concentration. Conducting real-time investigations into this problem is advantageous for further research, as it may lead to novel solutions for simultaneously testing salt concentration using a single PCF device.

The primary objective of our study was to simulate an optical salinity sensor based on a micro-structured fiber.

Salinity serves as a critical parameter in various fields, including oceanography [33], aquaculture [34], and water quality control [35]. Employing the Beam Propagation Method (BPM) simulation technique, we modeled the behavior of light within the micro-structured fiber and assessed its sensitivity to salinity. Through this simulation, we analyzed how light variations corresponded to changes in the salinity of the tested sample. The results obtained provided insights into the operational principles of the optical salinity sensor and allowed us to optimize its performance in terms of sensitivity and accuracy.

In this paper, we perform a numerical evaluation of a novel PCF comprised of four rings. The first ring is filled with seawater, and we analyze the sensor's performance by varying the diameter. This research contributes to the advancement of optical sensors by exploring a specific application in the field of salinity measurement. The results obtained could serve as a basis for the development of more sensitive and accurate sensors in this field, opening up new possibilities for monitoring and managing aquatic resources. Additionally, we demonstrate that this PCF sensor represents a viable option for dispersion-compensating fibers in optical communication links.

II. THEORY AND STRUCTURAL DESIGN

Our sensor is built on a photonic crystal fiber, as was indicated in the introduction. Figure 1(a) illustrates a cross section of our suggested sensor. Our PCF, which is measured 10000 µm of length, is formed of four rings airholes. seawater is introduced into the holes in the first ring. The relevant design parameters as indicated in Table 1, are the holes pitch (ʌ) which is the distance between the centers of two airholes, airholes diameter (d), and the diameter of the holes filled with seawater (d_1), while the substract of the structure is made by silica, is known as background material. The profile index of the PCF is presented in Fig. 2(b).

According to the Lorentz-Lorenz relationship, the refractive index (RI) of a substance is connected to its density and, consequently, to the presence of absolute salinity [34-36]. Thus, by measuring the refractive index of water level, we may determine the associated saltwater salinity. Seawater's RI changes depending on the excitation wavelength, salinity, and water temperature. The link between saltwater salinity, ambient seawater temperature, and seawater refractive index can be expressed as follows for a clearer understanding [29]:

$$n(S,T,\lambda) = 1.3140 + (1.779\times10^{-4} - 1.05\times 10^{-6}T + 1.6\times10^{-8}T^2)S - 2.02\times10^{-6}T^2 + \frac{15.868 + 0.01155S - 0.00423T}{\lambda} - \frac{4382}{\lambda^2} + \frac{1.1455\times10^{-6}}{\lambda^3} \quad . \quad (1)$$

Here, S is the concentration of salinity (% or PSU "practical salinity unit"), 1 PSU represents 1 gram of salt dissolved in 1 liter of water (g/l) [37] . T is the temperature (°C) of the salt water. We show the link between saltwater RI and the wavelengths at a constant temperature (30 °C). According to Fig. 2, rising the salinity concentration in the saltwater increases the RI. So, the effective refractive index has been employed to investigate the propagation properties of PCF. This is due to the fact that the effective index approach is a simple numerical methodology that yields qualitatively the same modal features as PCF.

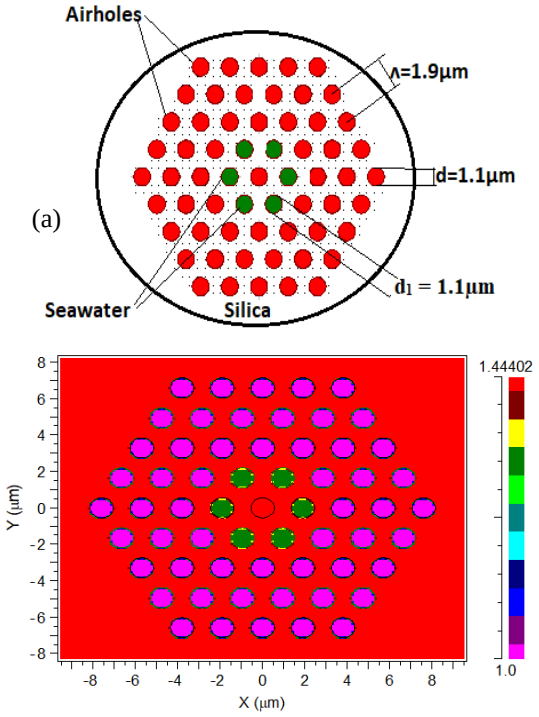

Fig. 1. (a) Model of the suggested PCF, (b) The profile index of the suggested PCF

TABLE 1
THE PARAMETERS OF THE STRUCTURED PCF

Parameters	Values
The period ʌ	1.9 µm
The diameter d	1.1 µm
The diameter d1	1.1 µm
Outer cladding diameter	125 µm
Coating diameter	245 µm

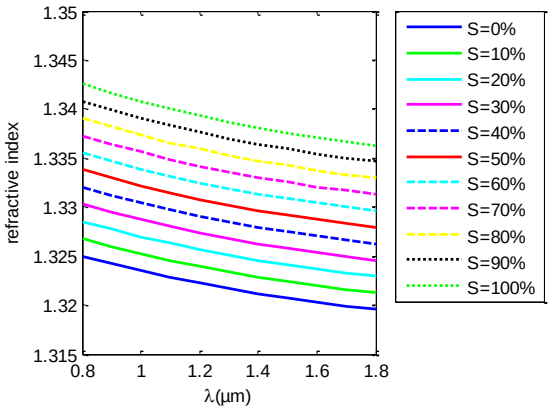

Fig. 2. The correlation between seawater refractive index (RI) and concentration of salinity in water.

To precisely simulate the guiding mode and examine sensor performance, Using Sellmeier's formula, the backdrop material's silica dispersion is taken into account [38]:

$$n^2(\lambda) = 1 + \frac{0.6961663\lambda^2}{\lambda^2 - (0.0684043)^2} + \frac{0.4079426\lambda^2}{\lambda^2 - (0.1162414)^2} + \frac{0.8974794\lambda^2}{\lambda^2 - (9.896161)^2}, \quad (2)$$

λ is the wavelength in µm. We utilized numerical techniques to analyze and investigate the chromatic dispersion properties of the sensor base PCF by taking into account the refractive index of pure silica.

III. RESULT AND DISCUSSION

A. First ring infiltrated with sea water

To achieve high sensitivity, we examined the dispersion characteristics of the proposed sensor using numerical modelling techniques. Figure 3 plots the behaviour of the chromatic dispersion in various concentrations (0-10-20-30-40-50-60-70-80-90 and 100) % of seawater in a scope of wavelength from 0.8µm to 1.8µm. At this stage, we have injected different concentrations of seawater in the first ring holes. By varying the concentration, the dispersion is calculated to observe the various results. It is clear that the dispersion shift with the changing of the concentration. So, dispersion is dependent on seawater concentrations. Meaning that our PCF is very attractive and sensitive to salinity. Furthermore, Chromatic dispersion is negative for a large scope of wavelengths, from 0.8 µm to about 1.6µm. These substantial negative dispersion values can be utilized to offset the typical dispersion of conventional single-mode fibers. This means that PCF can compensate for dispersion generated by conventional single-mode fiber. Thus, it can make our proposed salinity sensor suitable for communication application.

As mentioned earlier and based on the analyses presented above, it is evident that the refractive index of a solution is influenced by the salt content of the water.

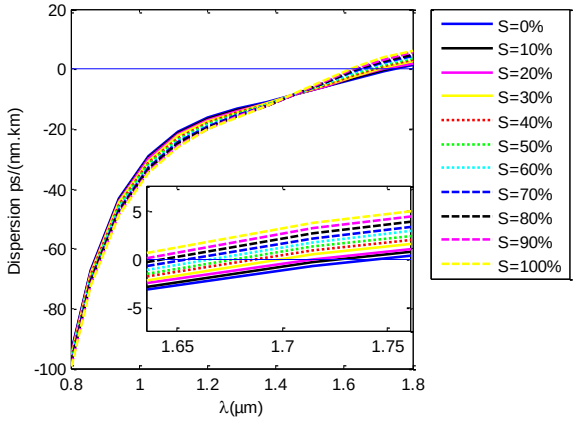

Fig. 3. The alteration in chromatic dispersion as a function of wavelength with various salt concentrations in water

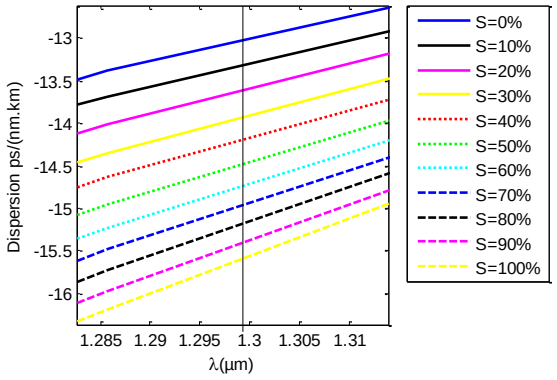

(a)

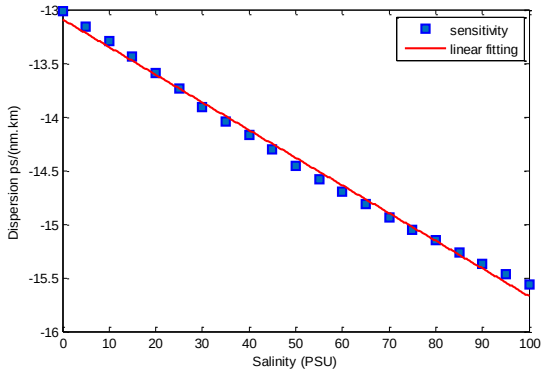

(b)

Fig. 4. (a) Variation of the chromatic dispersion at λ=1.3µm, (b) The calculated sensibility when λ=1.3µm

Therefore, the salinity can be indirectly determined by measuring the refractive index. Consequently, the salt concentration of the solution can be assessed by detecting the transmitted or reflected optical signal. To address potential issues related to salinity measurement, we calculated the salinity sensitivity of our PCF sensor at two wavelengths commonly used in optical fiber maintenance systems: 1.3 µm and 1.55 µm.

The sensitivity has an important role to evaluate the suggested sensor performs in terms of sensing, which can be defined as:

$$s\left(\frac{ps}{\frac{nmkm}{PSU}}\right) = \left|\Delta Dispersion(ps/(nmkm)) / \Delta Concentration(PSU)\right|. \quad (3)$$

Figure 4(a) represents the shift of chromatic dispersion at 1.3µm for different concentration of seawater. The salinity sensitivity was calculated and represented in Fig. 4(b). And the average sensitivity is 0.025805 ps/(nm.km)/PSU.

Figure 5(a) exhibits the behaviour of chromatic dispersion at λ=1.55µm. It was selected to determine the sensitivity of this sensor at this particular location. The sensitivity was calculated by applying the linear fitting and it can be computed to be 0.022247 ps/(nm.km)/PSU. The calculated sensitivity is presented in Fig. 5(b).

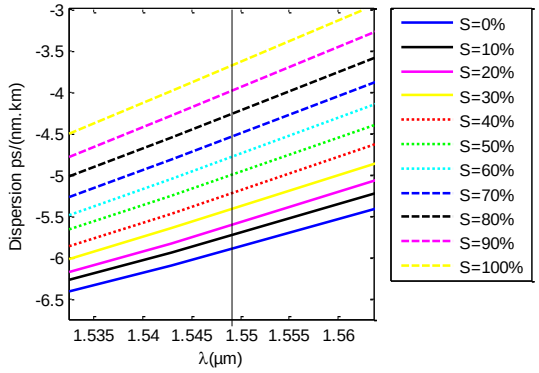

(a)

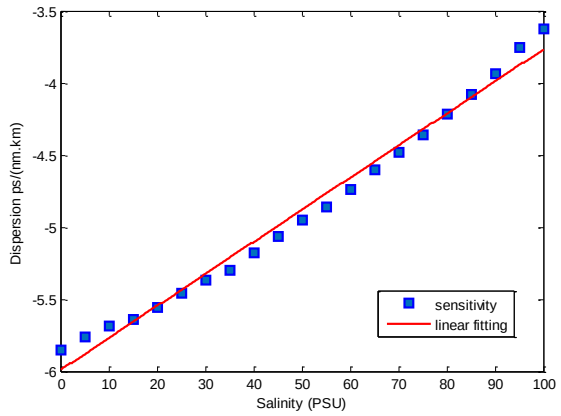

(b)

Fig. 5. (a) Variation of the chromatic dispersion at λ=1.55μ, (b) The calculated sensibility when λ=1.55μm

B.The effect of the opto-geometric parameter on sensing performance

As a way to modify and enhance the recommended PCF's sensing capabilities, the effect of modified an opto-geometric parameter is analyzed numerically. Figure 6(a) presents the cross view of the micro-structured PCF in which the diameter of the first ring holes was changed. In this structure, we keep the same parameters of the first PCF. The diameter of the holes, in the first ring, is d_2=0.6μm, which is filled with seawater. All the airholes diameters are d=1.1 μm and the variation in pitch between them is ʌ= 1.9μm. Using the Sellmeier's equation [38], The PCF's background is determined by the fused silica's computed chromatic dispersion. The profile index is shown in Fig. 6(b).

We utilized numerical methods to simulate the characteristics of the PCF. Figure 7 illustrates the effect of the change of chromatic dispersion. A slight change occurs when the salinity changes. So, there is a connection between the dispersion and the concentration of salt and the dispersion is dependent on the salinity demonstrating that the PCF may be used as a salinity sensor.

We investigate the effect of this modification in the structure. We simulate the chromatic dispersion at the same wavelengths chosen in the first section, 1.3μm and 1.55μm, the two telecommunication wavelengths. First, Fig. 8(a) plotted the shift of dispersion at 1.3μm for various concentration of seawater to calculate the sensitivity at this point. The performance of the sensor is significantly impacted by a change in the diameter of the initial ring holes, and the estimated results are shown in Fig. 8(b). The salinity sensitivity is obtained about 0.017966 ps/(nm.km)/PSU.

Then, the effect of the diameter of the first ring holes on dispersion is also investigated for the wavelength 1.55μm in Fig. 9(a). by applying a linear fitting in Fig. 9(b), the salinity sensitivity is obtained about 0.021818 ps/(nm.km)/PSU.

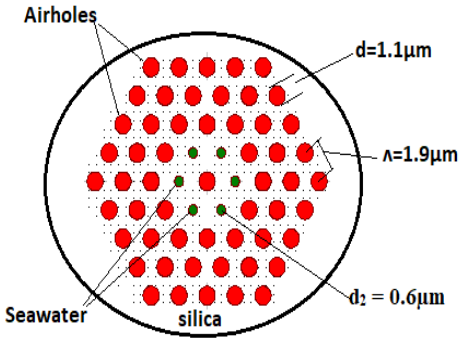

(a)

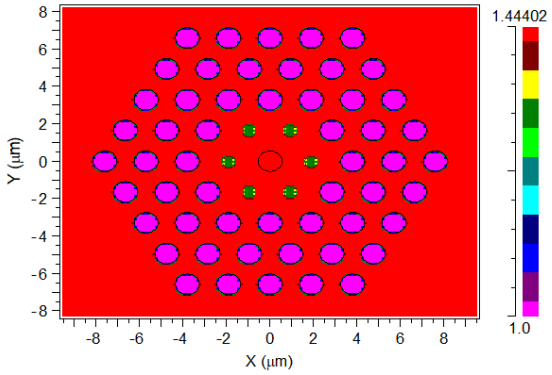

(b)

Fig. 6. (a) A model of the proposed PCF with a change of the diameter d_2, (b) The profile index of the structure

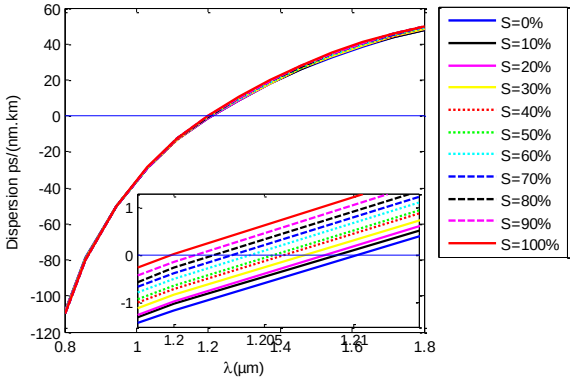

Fig. 7. The variation of the dispersion versus a scope of wavelengths from 0.8μm to 1.8μm with various salt level in water.

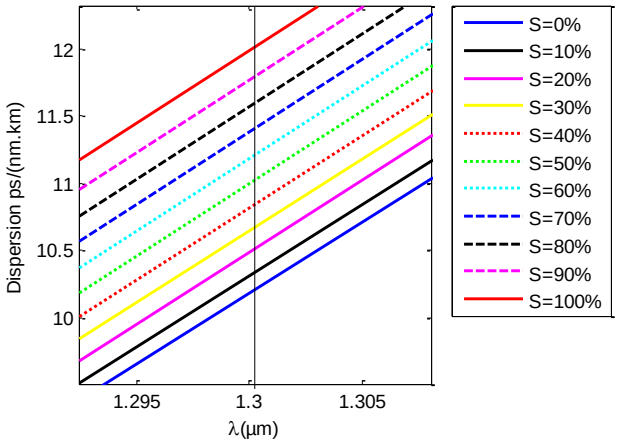

(a)

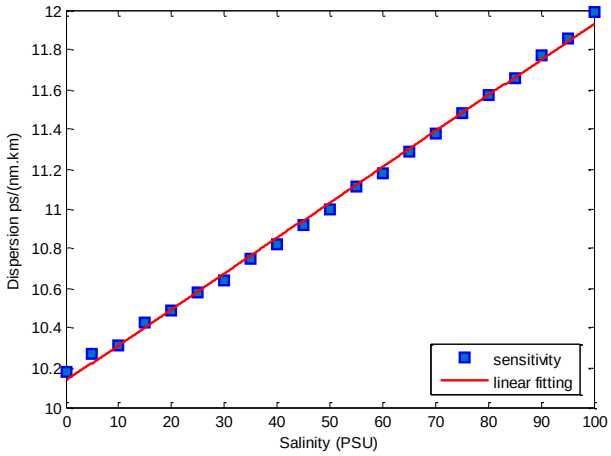

(b)

Fig. 8. (a) Variation of the chromatic dispersion at λ=1.3µm, (b) The calculated sensibility when λ=1.3µm

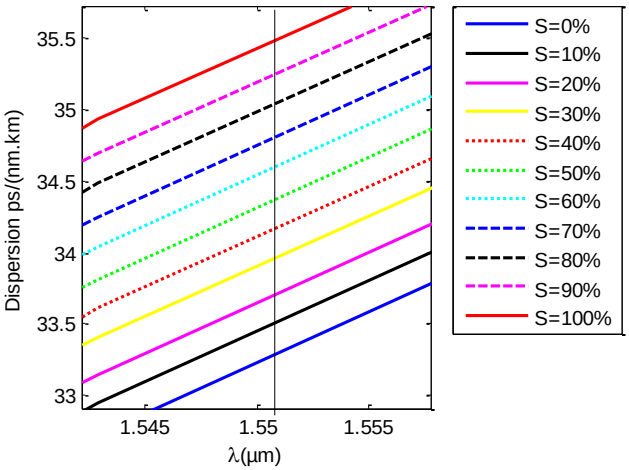

(a)

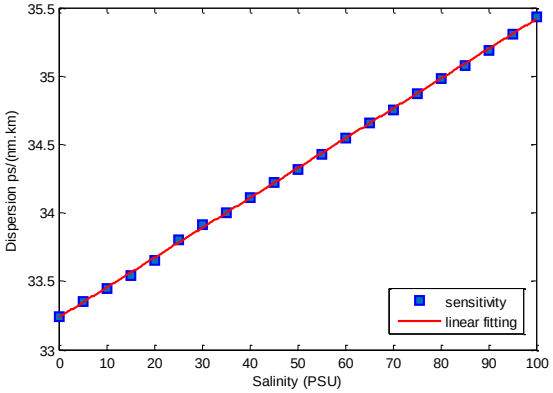

(b)

Fig. 9. (a) Variation of the chromatic dispersion at λ=1.55µm, (b) The calculated sensibility when λ=1.55µm

C. Multifunctionality of the photonic crystal fiber

It is crucial to investigate the impact of varying airhole diameters on the sensor's performance. Figures 10(a) and 10(b) show the schematics representation of the forming PCF and the profile index respectively. In this design, all airholes are spaced with a constant pitch of 1.9µm, and their diameter is 1.1µm. The first ring holes diameter is d_3=1.5µm where the salt water is injected. The sellmeier equation determines fused silica as the fiber's background material [38].

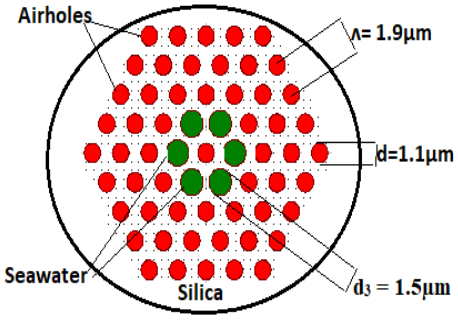

(a)

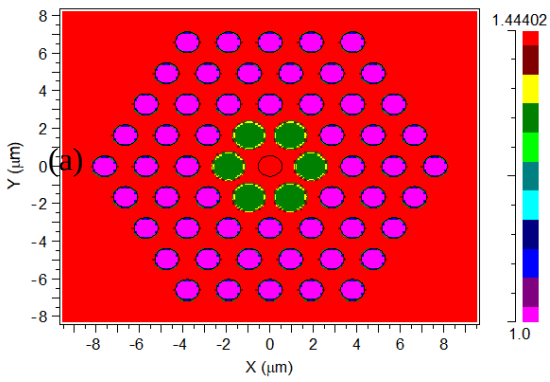

(b)

Fig. 10. (a) A cross section of the PCF when d3= 1.5µm, (b) The profile index of the structure

Figure 11 describes the shift of the chromatic dispersion versus wavelengths with various concentration of salinity in water. It is obvious that our sensor has a high sensitivity for detecting salinity. Besides, the chromatic dispersion is obviously negative, from 0.8μm to 1.8μm. These large negative dispersion values can be employed to compensate for the anomalous dispersion of conventional single mode fibers. It is obvious that an extremely negative dispersion may be attained along the telecommunication band for the optimal set of parameters, offering good dispersion compensation.

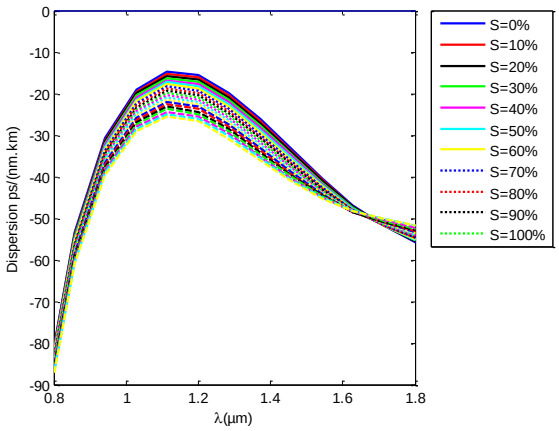

Fig. 11. The variation of the chromatic dispersion versus wavelength with various salt level in water

As previously, we choose two different wavelengths for determining the sensitivity of this salinity sensor: 1.3μm and 1.55μm, and we investigate the fluctuation of chromatic dispersion at each of these wavelengths.

Figure 12(a) represents the wavelength dependent characteristics of chromatic dispersion for various seawater concentrations at 1.3μm. From Fig. 12(b), the sensitivity is calculated by applying linear fitting and computed as 0.10815 ps/(nm.km)/PS.

The sensitivity is then calculated using the example when λ=1.55 μm. The variation of the chromatic dispersion is displayed in Fig. 13(a) and the computations were performed at a fixed wavelength (1.55 μm) as indicated in Fig. 13(b). Using the linear fitting, the average value for salinity sensitivity may be determined to be 0.0455964 ps/(nm.km)/PSU based on the measured experimental data.

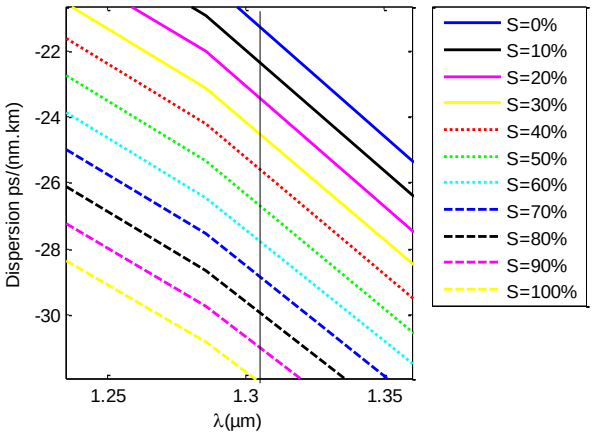

(a)

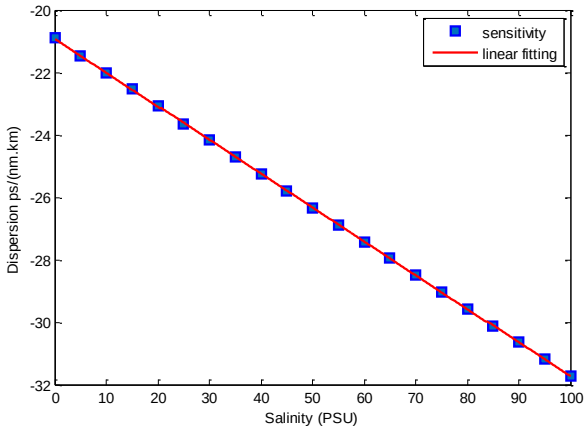

(b)

Fig. 12. (a) Variation of the chromatic dispersion at λ=1.3μm, (b) The calculated sensibility when λ=1.3μm

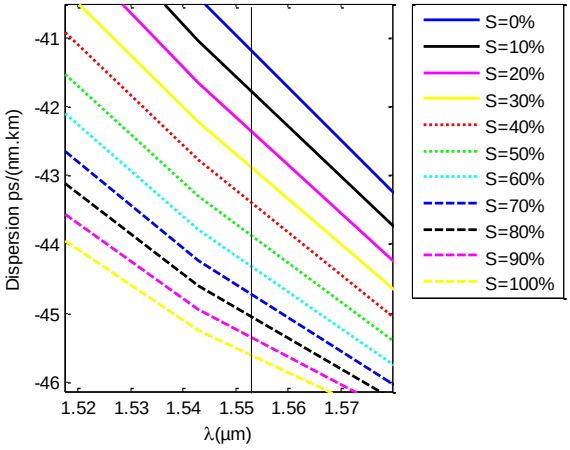

(a)

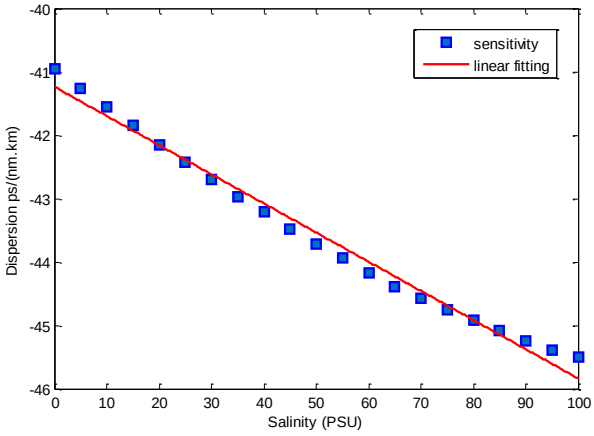

(b)

Fig. 13. (a) Variation of the chromatic dispersion at λ=1.55μm, (b) The calculated sensibility when λ=1.55μm

As we showed in the previous section, by computing the dispersion, we can easily calculate the salinity sensitivity by varying the salt concentration from 0% to 100%. We analyze the performance of our proposed sensor. We examined three different structure and calculate sensitivity for two wavelengths 1.3 μm and 1.55 μm. Table 2 presents the results

obtained from previous simulation according the shift of dispersion.

TABLE 2
THE RESULT OF THE SENSITIVITIES FOR DIFFERENT WAVELENGTHS

Structure	Wavelengths	Sensitivity (ps/(nm.km)/PSU)
Λ=1.9 μm d=1.1 μm d_1=1.1 μm	1.3 μm	0.025805
	1.55 μm	0.022247
Λ =1.9 μm d=1.1 μm d_2= 0.5 μm	1.3 μm	0.017966
	1.55 μm	0.021818
Λ =1.9 μm d=1.1 μm d_3=1.5 μm	1.3 μm	0.10815
	1.55 μm	0.045964

For different salt concentrations in water, the highest sensitivity when λ=1.3μm is 0.017966 ps/(nm.km)/PSU and when λ=1.55μm is 0.021818 ps/(nm.km)/PSU. So, the greatest sensitivity to varied salt concentrations can be modified by adjusting the PCF design parameters.

Table 3 presents a summary of some previously documented salinity sensors along with their respective sensitivities, the structure of our PCF is simple and commonly used, suggesting that fabrication should be straightforward.

Finally, and based on the above results of our research, it can be improved that the change of one parameter in the structure is important to have better results. This sensor has a low cost and simple structure. Therefore, the suggested sensor may be employed for salinity sensing when its parameters are improved. Additionally, the suggested sensor can be utilized as a multipurpose tool, a sensor, to measure salinity or as a PCF for low-loss communication.

TABLE 3
VARIOUS SENSITIVITY COMPARISON AMONG DIFFERENT SALINITY SENSOR

Structures	S pm/%	S nm/RIU	S ps/(nm.km)/ PSU	Ref.
Sea water salinity sensing	30	-	-	[39]
Salinity sensing based on MKR	21.18	-	-	[40]
Salinity sensor using PCF	-	5675	-	[29]
Salinity sensor based on sagnac interformeter	-	37,500	-	[33]
This work	-	-	0.017966 at 1.3μm 0.021818 at 1.55μm	-

IV. CONCLUSION

This paper aimed to elucidate a proposed salinity sensor that would employ photonic crystal fiber and be numerically modeled. The sensor's salinity detection range spanned from 0% to 100%. Seawater was introduced into the first ring holes, which served as defect cores in the fiber. The influence of structural parameters on the sensor's performance was explored by varying the diameter of the first ring holes. The simulation results revealed that the highest salinity sensitivity was achieved at 1.3μm, amounting to 0.017966 ps/(nm.km)/PSU, and at 1.55μm, the sensitivity was 0.021818 ps/(nm.km)/PSU. Furthermore, the dispersion properties of PCFs were examined, showcasing their significant negative chromatic dispersion, rendering them valuable for dispersion-compensating applications. In conclusion, the results underscore the feasibility of the simulated PCF for salinity sensing applications and its potential use in optical communication by a simple change in geometric parameters, particularly concerning chromatic dispersion-related needs.

REFERENCES

[1] J. Heikenfeld *et al.*, "Wearable sensors: modalities, challenges, and prospects," *J Lab on a Chip*, vol. 18, no. 2, pp. 217-248, 2018., DOI: 10.1039/C7LC00914C.

[2] Y. Kularia, S. Kohli, and P. P. Bhattacharya, "Analyzing propagation delay, transmission loss and signal to noise ratio in acoustic channel for Underwater Wireless Sensor Networks," *IEEE 1st international conference on power electronics, intelligent control and energy systems (ICPEICES)*, pp. 1-5: , 2016, DOI: 10.1109/ICPEICES.2016.7853300.

[3] M. Panahi-Sarmad et al., "A comprehensive review on carbon-based polymer nanocomposite foams as electromagnetic interference shields and piezoresistive sensors," *J ACS Applied Electronic Materials*, vol. 2, no. 8, pp. 2318-2350, 2020. DOI: 10.1021/acsaelm.0c00490.

[4] L. Wang et al., "Application challenges in fiber and textile electronics," *J Advanced Materials*, vol. 32, no. 5, p. 1901971, 2020. DOI: 10.1002/adma.201901971.

[5] H. K. Hisham, "Optical fiber sensing technology: basics, classifications and applications," *J American Journal of remote sensing*, vol. 6, no. 1, pp. 1-5, 2018. DOI: 10.11648/j.ajrs.20180601.11.

[6] H.-E. Joe, H. Yun, S.-H. Jo, M. B. Jun, and B.-K. Min, "A review on optical fiber sensors for environmental monitoring," *J International journal of precision engineering manufacturing-green technology*, vol. 5, pp. 173-191, 2018. DOI: 10.1007/s40684-018-0017-6.

[7] M. F. Ferreira et al., "Roadmap on optical sensors," *J Journal of Optics*, vol. 19, no. 8, p. 083001, 2017., DOI: 10.1088/2040-8986/aa7419.

[8] B. Troia, A. Paolicelli, F. De Leonardis, and V. M. Passaro, "Photonic crystals for optical sensing: A review," *J Advances in Photonic Crystals*, pp. 241-295, 2013, DOI: 10.5772/53897.

[9] X. Luo et al., "High-sensitivity dual U-shaped PCF-SPR refractive index sensor for the detection of gas and liquid analytes," *J JOSA A*, vol. 41, no. 4, pp. 595-605, 2024. DOI: 10.1364/JOSAA.514808.

[10] M. De, T. K. Gangopadhyay, and V. K. Singh, "Prospects of photonic crystal fiber as physical sensor: An overview," *J Sensors*, vol. 19, no. 3, p. 464, 2019.DOI: 10.3390/s19030464.

[11] F. A. Mou, M. M. Rahman, M. R. Islam, M. I. H. J. S. Bhuiyan, and B.-S. Research, "Development of a photonic crystal fiber for THz wave guidance and environmental pollutants

detection," *J Sensing Bio-Sensing Research*, vol. 29, p. 100346, 2020. DOI: 10.1016/j.sbsr.2020.100346.
[12] Z. Li et al., "The polarization crossfire (PCF) sensor suite focusing on satellite remote sensing of fine particulate matter PM2. 5 from space," *J Journal of Quantitative Spectroscopy Radiative Transfer*, vol. 286, p. 108217, 2022. DOI: 10.1016/j.jqsrt.2022.108217.
[13] I. Mired, M. Debbal, and H. Chikh-Bled, "Pressure Sensing Based on Photonic Crystal Fiber by Infiltrating the Air-Holes with Water," *J Progress in Electromagnetics Research C*, vol. 130, 2023., DOI: 10.2528/PIERC22122503.
[14] M. Debbal, M. Bouregaa, H. Chikh-Bled, M. E. K. Chikh-Bled, and M. C. E. Ouadah, "Influence of temperature on the chromatic dispersion of photonic crystal fiber by infiltrating the air holes with water," *J Journal of Optical Communications*, vol. 44, no. 2, pp. 163-166, 2023., DOI: 10.1515/joc-2019-0074.
[15] A. Z. Mohammed, "Photonic crystal fiber Mach-Zehnder interferometer pH sensing," *AIP conference proceedings*, vol. 2045, no. 1, p. 020010, 2018, DOI: 10.1063/1.5080823.
[16] M. Y. Azab, M. F. O. Hameed, A. M. Nasr, and S. Obayya, "Label free detection for DNA hybridization using surface plasmon photonic crystal fiber biosensor," *J Optical Quantum Electronics*, vol. 50, pp. 1-13, 2018. DOI: 10.1007/s11082-017-1302-2.
[17] A. Kumar, P. Verma, and P. Jindal, "Photonic Crystal Fiber Based Refractive Index Sensor for Cholesterol Sensing in Far Infrared Region," in *Advances in Data Computing, Communication and Security: Proceedings of I3CS2021*: Springer, 2022, pp. 533-542, DOI: 10.1007/978-981-16-8403-6_49.
[18] H. Thenmozhi, M. M. Rajan, V. Devika, D. Vigneswaran, and N. Ayyanar, "D-glucose sensor using photonic crystal fiber," *J Optik*, vol. 145, pp. 489-494, 2017, DOI: 10.1016/j.ijleo.2017.08.039
[19] V. Budinski and D. Donlagic, "Fiber-optic sensors for measurements of torsion, twist and rotation: a review," J Sensors, vol. 17, no. 3, p. 443, 2017, DOI: 10.3390/s17030443.
[20] Y. Guo, M. Chen, L. Xiong, X. Zhou, and C. Li, "Fiber Bragg grating based acceleration sensors: a review," *J Sensor Review*, 2021, DOI: 10.1108/SR-10-2020-0243.
[21] A. Leymonerie, J.-S. Boisvert, L. Juszczak, and S. Loranger, "Enhanced sensitivity distributed sensing of magnetic fields in optical fiber using random Bragg grating," *J Optics Continuum*, vol. 3, no. 1, pp. 94-101, 2024, DOI: 10.1364/OPTCON.509943.
[22] C. Li et al., "Integrated fiber-optic Fabry–Perot vibration/acoustic sensing system based on high-speed phase demodulation," *J Optics Laser Technology*, vol. 169, p. 110131, 2024, DOI: 10.1016/j.optlastec.2023.110131.
[23] A. Mahlooji and F. Azhari, "A Fiber-Only Optical Vibration Sensor Using Off-Centered Fiber Bragg Gratings," in *IEEE Sensors Journal*, vol. 24, no. 9, pp. 14245-14252, 2024, DOI: 10.1109/JSEN.2024.3370841.
[24] Z. Zhao, M. Tang, and C. Lu, "Distributed multicore fiber sensors," *J Opto-Electronic Advances*, vol. 3, no. 2, pp. 190024-1-190024-17, 2020, DOI: 10.29026/oea.2020.190024.
[25] M. Scaioni, M. Marsella, M. Crosetto, V. Tornatore, and J. Wang, "Geodetic and remote-sensing sensors for dam deformation monitoring," *J Sensors*, vol. 18, no. 11, p. 3682, 2018, DOI: 1424-8220/18/11/3682.
[26] N. S. Rahim and S. S. Al-Bassam, "Photonic crystal fiber Fabry–Perot interferometer for humidity sensor," *J Journal of Optics*, pp. 1-6, 2024, DOI: 10.1007/s12596-023-01604-0.
[27] M. Yunus and A. Arifin, "Design of oil viscosity sensor based on plastic optical fiber," in *Journal of Physics: Conference Series*, 2018, vol. 979, no. 1, p. 012083: IOP Publishing, DOI: 10.1088/1742-6596/979/1/012083.
[28] A. I. Ferdous et al., "High-sensitivity chemical sensing and detection applications based on octagonal-shaped hybrid photonic crystal fiber with a hexagonal core," *J Journal of Optics*, pp. 1-13, 2024, DOI: 10.1007/s12596-024-01654-y.
[29] D. Vigneswaran, N. Ayyanar, M. Sharma, M. Sumathi, M. Rajan, and K. Porsezian, "Salinity sensor using photonic crystal fiber," *J Sensors Actuators A: Physical*, vol. 269, pp. 22-28, 2018. DOI: 10.1016/j.sna.2017.10.052.
[30] K. Ramya, Y. E. Monfared, R. Maheswar, and V. Dhasarathan, "Dual-core twisted photonic crystal fiber salinity sensor: a numerical investigation," *J IEEE Photonics Technology Letters*, vol. 32, no. 10, pp. 616-619, 2020, DOI: 10.1109/LPT.2020.2987949.
[31] V. Chaudhary, P. Gaur, and S. Rustagi, "Sensors, society, and sustainability," *J Sustainable Materials Technologies*, p. e00952, 2024, DOI: 10.1016/j.susmat.2024.e00952.
[32] S. Ma et al., "Relative Humidity Sensing Based on Passively Mode-Locked Fiber Laser With Polyimide-Coated Fiber," in *IEEE Sensors Journal*, vol. 24, no. 5, pp. 6257-6263, 2024, DOI: 10.1109/JSEN.2024.3352616.
[33] M. A. Mollah, M. Yousufali, M. R. B. A. Faysal, M. R. Hasan, M. B. Hossain, and I. Amiri, "Highly sensitive photonic crystal fiber salinity sensor based on Sagnac interferometer," *J Results in Physics*, vol. 16, p. 103022, 2020, DOI: 10.1016/j.rinp.2020.103022.
[34] X. Zhang and W. Peng, "Temperature-independent fiber salinity sensor based on Fabry-Perot interference," *J Optics express*, vol. 23, no. 8, pp. 10353-10358, 2015, DOI: 10353-10358
[35] X. Wang, J. Wang, S.-S. Wang, and Y.-P. Liao, "Fiber-optic salinity sensing with a panda-microfiber-based multimode interferometer," *J Journal of Lightwave Technology*, vol. 35, no. 23, pp. 5086-5091, 2017, DOI: 10.1109/JLT.2017.2764743.
[36] W. Xu et al., "All-fiber seawater salinity sensor based on fiber laser intracavity loss modulation with low detection limit," *J Optics Express*, vol. 27, no. 2, pp. 1529-1537, 2019, DOI: 10.1364/OE.27.001529.
[37] Y. Qian, Y. Zhao, Q.-l. Wu, Y. J. S. Yang, and A. B. Chemical, "Review of salinity measurement technology based on optical fiber sensor," vol. 260, pp. 86-105, 2018. DOI: 10.1016/j.snb.2017.12.077.
[38] E. K. Akowuah, T. Gorman, H. Ademgil, S. Haxha, G. K. Robinson, and J. V. Oliver, "Numerical analysis of a photonic crystal fiber for biosensing applications," *J IEEE Journal of Quantum Electronics*, vol. 48, no. 11, pp. 1403-1410, 2012, DOI: 10.1109/JQE.2012.2213803.
[39] G.-X. Li, J. Wang, H.-J. Yang, Z.-T. Su, and S.-S. Wang, "Simulation study of microring resonator for seawater salinity sensing with weak temperature dependence," *J The European Physical Journal-Applied Physics*, vol. 68, no. 2, p. 20502, 2014, DOI: 10.1051/epjap/2014140218.
[40] Y. Liao, J. Wang, H. Yang, X. Wang, and S. Wang, "Salinity sensing based on microfiber knot resonator," *J Sensors Actuators A: Physical*, vol. 233, pp. 22-25, 2015, DOI: 10.1016/j.sna.2015.06.019.